Table 3. *Interatomic distances and angles in salesite,* $CuIO_3(OH)$

| | | |
|---|---|---|
| **Within the iodate group** | | |
| $I-O_1$ | $1{\cdot}78 \pm 0{\cdot}09$ Å | |
| $I-O_2$ | $1{\cdot}82 \pm 0{\cdot}05$ | (×2) |
| $O_1-O_2$ | $2{\cdot}75 \pm 0{\cdot}10$ | (×2) |
| $O_2-O_2''$ | $2{\cdot}70 \pm 0{\cdot}07$ | |
| $O_1-I-O_2$ | $97{\cdot}2 \pm 2{\cdot}1°$ | (×2) |
| $O_2-I-O_2''$ | $95{\cdot}6 \pm 1{\cdot}4$ | |
| $O_1-O_2-O_2''$ | $60{\cdot}7 \pm 1{\cdot}5$ | (×2) |
| $O_2-O_1-O_2''$ | $58{\cdot}7 \pm 1{\cdot}5$ | |
| **Within the copper octahedron** | | |
| Cu–(OH) | $1{\cdot}95 \pm 0{\cdot}07$ Å | (×2) |
| $Cu-O_2$ | $2{\cdot}01 \pm 0{\cdot}05$ | (×2) |
| $Cu-O_1'$ | $2{\cdot}59 \pm 0{\cdot}09$ | (×2) |
| $O_2$–(OH) | $2{\cdot}68 \pm 0{\cdot}09$ | (×2) |
| $O_2$–(OH)′ | $2{\cdot}91 \pm 0{\cdot}09$ | (×2) |
| $O_1'-O_2'$ | $3{\cdot}37 \pm 0{\cdot}10$ | (×2) |
| $O_1'-O_2$ | $3{\cdot}16 \pm 0{\cdot}10$ | (×2) |
| $O_1'$–(OH)′ | $2{\cdot}75 \pm 0{\cdot}11$ | (×2) |
| $O_1'$–(OH) | $3{\cdot}53 \pm 0{\cdot}11$ | (×2) |
| (OH)-Cu-$O_2$ | $82{\cdot}5 \pm 1{\cdot}5°$ | (×2) |
| (OH)′-Cu-$O_2$ | $97{\cdot}5 \pm 1{\cdot}5$ | (×2) |
| $O_1'$-Cu-$O_2$ | $84{\cdot}6 \pm 1{\cdot}6$ | (×2) |
| $O_1'$-Cu-$O_2'$ | $95{\cdot}4 \pm 1{\cdot}6$ | (×2) |
| $O_1'$-Cu-(OH) | $101{\cdot}3 \pm 1{\cdot}8$ | (×2) |
| $O_1'$-Cu-(OH)′ | $78{\cdot}7 \pm 1{\cdot}8$ | (×2) |
| **Non-bonded I-O distances** | | |
| I–(OH) | $2{\cdot}50 \pm 0{\cdot}07$ Å | |
| $I-O_2''''$ | $2{\cdot}69 \pm 0{\cdot}05$ | |

der wissenschaftlichen Forschung for a grant. He is grateful to Pauline K. Persing Ghose for much technical assistance and for the diagrams.

## References


AEBI, F. (1948). *Helv. Chim. Acta*, **31**, 369.

BERGHUIS, J., HAANAPPEL, IJ. M., POTTERS, M., LOOPSTRA, B. O., MACGILLAVRY, C. H. & VEENENDAAL, A. L. (1955). *Acta Cryst.* **8**, 478.

COCCO, G. & MAZZI, F. (1959). *Period. d. Miner.* **28**, 121.

CROMER, D. T. & LARSON, A. C. (1956). *Acta Cryst.* **9**, 1015.

*Dana's System of Mineralogy* (1951), 7th ed., vol. 2. p. 316. New York: Wiley.

FORSYTH, J. B. & WELLS, M. (1959). *Acta Cryst.* **12**, 412.

GRANGER, A. & DE SCHULTEN, A. (1904). *Bull. Soc. Min. Franç.* **27**, 137.

IBERS, J. A. (1956). *Acta Cryst.* **9**, 225.

IITAKA, Y. (1961). Unpublished.

JAMES, R. W. & BRINDLEY, G. W. (1931). *Phil. Mag.* (7), **12**, 81.

LARSON, A. C. & CROMER, D. T. (1961). *Acta Cryst.* **14**, 128.

MACGILLAVRY, C. H. & VAN ECK, C. L. P. (1943). *Rec. Trav. Chim. Pays-Bas*, **62**, 729.

NÁRAY SZABÓ, I. & NEUGEBAUER, J. (1947). *J. Amer. Chem. Soc.* **69**, 1280.

NOWACKI, W. & SCHEIDEGGER, R. (1952). *Helv. Chim. Acta*, **35**, 375.

PALACHE, C. & JARRELL, O. W. (1939). *Amer. Min.* **24**, 388.

ROGERS, M. T. & HELMHOLZ, L. (1941). *J. Amer. Chem. Soc.* **63**, 278.

VIERVOLL, H. & ØGRIM, O. (1949). *Acta Cryst.* **2**, 277.

VORONOVA, A. A. & VAINSHTEIN, B. K. (1958). *Kristallografiya*, **3**, 444.

ZACHARIASEN, W. H. & BARTA, F. A. (1931). *Phys. Rev.* **37**, 1626.


*Acta Cryst.* (1962). **15**, 1109

# Stacking Fault in Precipitated Cadmium Sulphide

BY RYOITIRO SATO

*Mitsubishi Metal Mining and Metallurgical Laboratory, Omiya City, Saitama Prefecture, Japan*

(*Received* 10 *August* 1961)

In order to throw light upon the nature of stacking fault in precipitated cadmium sulphide, the crystals precipitated in epitaxial orientation on to the galena cleavage face are investigated by means of the electron diffraction reflexion method. It was reported already (Sato, 1959) that the structure of the precipitate is determined mainly by the composition of the aqueous solution of cadmium salt, from which the crystal is precipitated. In the present study, intensity distributions in diffraction patterns of many precipitates obtained with various cadmium salt solutions are dealt with in detail. The conclusions are (1) that the stacking faults observed in precipitated cadmium sulphide are 'growth faults', (2) that the 'Reichweite' of the growth necessary and sufficient for interpretation of the experimental results is 3, and (3) that the 'growth faults' in precipitated cadmium sulphide arise invariably in such a way that the faulty sequences, hex. → cub. and cub. → hex., are comparatively rare.

## 1. Introduction

In the course of electron diffraction investigations of metathetical actions of a number of aqueous solutions of heavy metal salts upon a number of sulphide mineral surfaces (Sato, 1953*a*, *b*, 1954, 1955, 1957), cadmium sulphide in epitaxial orientation has been obtained on the cleavage face of galena (PbS; NaCl-type cubic) treated with cadmium salt solutions. The function of galena in this surface reaction lies, first, in supplying

sulphur ions to the solution by dissolving, leading to the precipitation of cadmium sulphide, and, secondly, in assigning an expitaxy to the precipitate.

Because of the presence of epitaxy, the electron diffraction reflexion method will be effective in throwing light upon the structure of the cadmium sulphide precipitates. Thus, a previous report (Sato, 1959) showed (1) that, in accordance with Milligan (1934), hexagonal $\alpha$-CdS (greenockite; wurtzite-type) tends to be precipitated from cadmium halide solutions and cubic $\beta$-CdS (hawleyite after Traill & Boyle (1955); zinc blende-type) from cadmium nitrate and sulphate solutions, (2) that a certain mixture of, for example, cadmium chloride and nitrate solutions leads to one-dimensionally disordered cadmium sulphide, and (3) that the composition of the cadmium salt solution used is more essential than initial nuclei for crystallization in determining the atomic structure of precipitated cadmium sulphide. The present study is concerned with the nature of this one-dimensional disorder.

In the structures of cadmium sulphide the cadmium atoms (also the sulphur) are related, one to the other, as are the centres of a close-packed lattice, and a cadmium atom is tetrahedrally surrounded by four sulphur atoms, and *vice versa*. Therefore, faults in stacking of the hypothetical unit layers, each consisting of a Cd- and an S-plane, are expected to arise during growth, deformation or transformation of cadmium sulphide. Such a situation is analogous to that in the structures of zinc sulphide and silicon carbide.

The lattice constants of $\alpha$-CdS are $a=4{\cdot}136$, $c=6{\cdot}713$ Å (Swanson *et al.*, 1955). The ratio of the height of the elementary tetrahedron to the edge length of its basal triangle amounts to $6{\cdot}713/(2\times 4{\cdot}136)=0{\cdot}8116$, which shows only a slight deviation from the ideal value of $\sqrt{2}/\sqrt{3}=0{\cdot}8165$. The lattice constant of $\beta$-CdS is $a=5{\cdot}82$ Å (Wyckoff, 1960). The edge length of the elementary tetrahedron amounts to $(1/\sqrt{2})\times 5{\cdot}82$ Å $=4{\cdot}12$ Å, which is approximately equal to the $a$-value of $\alpha$-CdS. In the following, therefore, it will be assumed that $\alpha$-, $\beta$-, and also one-dimensionally disordered CdS are all composed of the same 'unit layers'.

## 2. Experimental

The fresh cleavage face of galena, $\{001\}_{\mathrm{PbS}}$, about 3 mm. × 3 mm. in size, was immersed in a cadmium salt solution. The cadmium salts used were $CdCl_2.(5/2)H_2O$, $CdBr_2.4H_2O$, $Cd(NO_3)_2.4H_2O$ and $CdSO_4.(8/3)H_2O$, all having satisfactory analyses.

Since preliminary experiments had shown that wide variations in the cadmium concentration and the temperature of the solution, and in the duration of the exposure of the specimen to the solution do not modify experimental results essentially, these experimental conditions were almost invariably chosen as 0·1 N, room temperature, and ½–20 hr., respectively. As for the pH value of the solution, $\mathrm{pH}<2{\cdot}5$ was necessary in order to make the metathetical reaction, $\mathrm{PbS}+\mathrm{Cd}^{++}\rightarrow\mathrm{CdS}+\mathrm{Pb}^{++}$, proceed to a considerable extent. Therefore, pH of the solution was invariably adjusted to $1{\cdot}7\pm 0{\cdot}1$ with the inorganic acid, which has the anion of the cadmium salt used.

For preparation of a mixture of two kinds of cadmium salt solutions, one favouring $\alpha$-CdS and the other $\beta$-CdS, the desired volumes of the two solutions prepared beforehand as above were mixed; the resulting mixture was, therefore, invariably 0·1 N in cadmium concentration and $1{\cdot}7\pm 0{\cdot}1$ in pH. In order to denote the ratio of the volumes to be mixed, the notations, $[NO_3]/[Cl]$, $[NO_3]/[Br]$, $[SO_4]/[Cl]$ and $[SO_4]/[Br]$, will be used; these notations imply also the ratios of the concentrations of the two kinds of anions (in normality) in the mixture.

After taking out of the solution, simple or mixed, the specimen was rinsed with water, and then inspected by electron diffraction (40 kV.; camera length, 30 cm.).

## 3. Results

In the previous report (Sato, 1959), several remarkable features in the experimental results were briefly touched upon. Since each of them requires a separate interpretation, here are presented only those results that have more or less direct bearings on the present concern, i.e. the nature of stacking fault in cadmium sulphide precipitate.

(1) To begin with, an example of electron micrograph of galena cleavage face treated slightly with cadmium salt solution is reproduced in Fig. 1. It is seen that the cadmium sulphide resulting from the metathetical reaction does not form a uniform film; it seems that precipitated particles decorate imperfections at the surface of the substrate. The diameter of the particles seems to be about 100 Å.

(2) With cadmium chloride or bromide solutions, $\alpha$-CdS is formed (Figs. 2 and 3). In its dominant epitaxy (1, 2, 3 and 4 in Fig. 4) the $c$-axes (polar axes) are approximately parallel to $\langle 111\rangle_{\mathrm{PbS}}$ and the $a$-axes are parallel to $\langle 110\rangle_{\mathrm{PbS}}$. This is expressed as

$$(03\bar{3}4)_{\alpha\text{-CdS}} \text{ approximately } // \{001\}_{\mathrm{PbS}}$$
$$[100]_{\alpha\text{-CdS}} // \langle 110\rangle_{\mathrm{PbS}} .$$

Although the former parallelism shows a slight deviation (about 2° at most), it becomes strict when a small amount of nitrate or sulphate is added to the solution. Sometimes a less dominant epitaxy (5 and 6 in Fig. 4) is observed in addition. In it the $c$-axes stand upright on the cleavage face and the $a$-axes are parallel to $\langle 110\rangle_{\mathrm{PbS}}$; i.e.

$$(0001)_{\alpha\text{-CdS}} // \{001\}_{\mathrm{PbS}}$$
$$[100]_{\alpha\text{-CdS}} // \langle 110\rangle_{\mathrm{PbS}} .$$

(3) With cadmium nitrate or sulphate solutions,

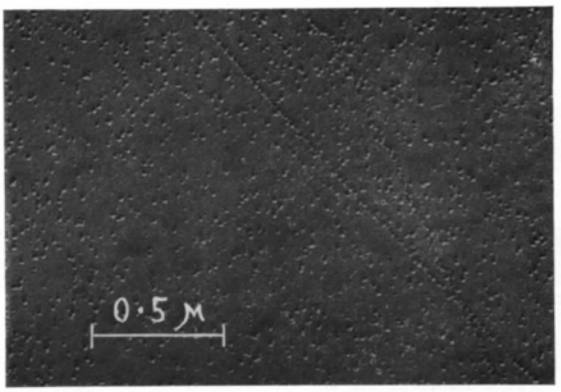


Fig. 1. Example of electron micrograph of galena cleavage face treated with cadmium salt solution. Treatment of substrate: $Cd(NO_3)_2$ 0·1 N, pH 1·7, room temperature, 5 min. One-stage carbon replication followed by shadowing with chromium.

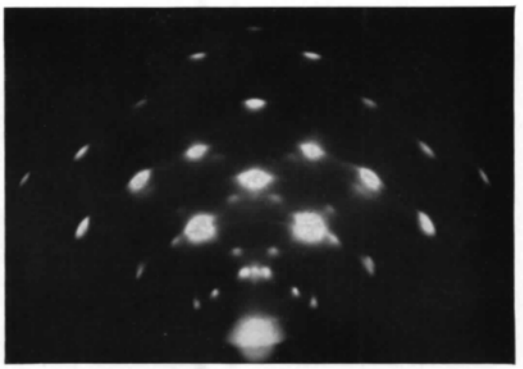

Fig. 2. Electron diffraction pattern of α-CdS formed on galena cleavage face. Treatment of substrate: $CdCl_2$ 0·1 N, pH 1·7, room temperature, 20 hr. Beam along $\langle 110 \rangle_{PbS}$.

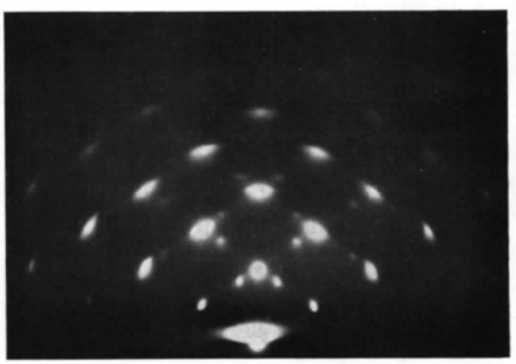

Fig. 5. Electron diffraction pattern of β-CdS formed on galena cleavage face. Treatment of substrate: $Cd(NO_3)_2$ 0·1 N, pH 1·7, room temperature, 20 hr. Beam along $\langle 110 \rangle_{PbS}$.

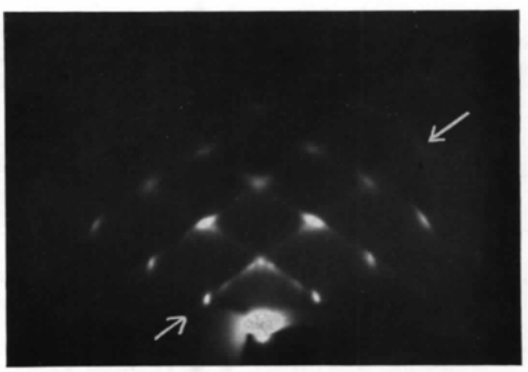

Fig. 7. Example of electron diffraction pattern of CdS involving stacking faults. Spot elongations due to stacking faults along, for example, the line marked $(h-k=-1)$ are noticeable. Treatment of substrate: cadmium concentration 0·1 N, $[NO_3]/[Cl]=75$, pH 1·7, room temperature, 20 hr.

[*To face p.* 1110

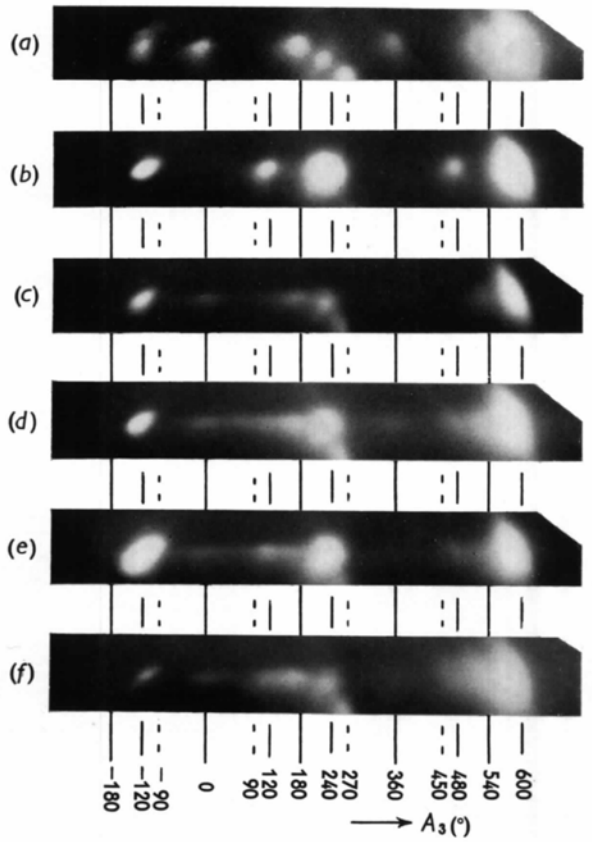


Fig. 8. Diffraction spots on the line with $h-k=-1$ (the line marked in Fig. 7). The abscissa, $A_3=360°\times l$, refers to the 'unit layer'. Treatments of substrates: for each, cadmium concentration 0·1 N, pH 1·7, room temperature, 20 hr.; (*a*) $[NO_3]/[Cl]=0$, (*b*) $[NO_3]/[Cl]=\infty$, (*c*) $[NO_3]/[Cl]=75$, (*d*) $[NO_3]/[Br]=75$, (*e*) $[NO_3]/[Br]=100$, and (*f*) $[SO_4]/[Cl]=3$.

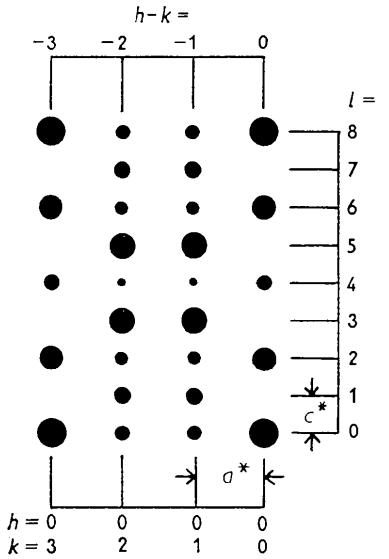


Fig. 3. Reciprocal lattice points of α-CdS. The plane of paper is $(2\bar{1}\bar{1}0)$. The areas of circles represent relative intensities calculated from the structure factor, where the scattering factors of Cd and S are both assumed to be constant and proportional to their atomic numbers. Note that *hkl* are the ordinary hexagonal indices; to convert them into the 'unit-layer hexagonal indices' (see Section 3, (5)), divide *l* by 2.

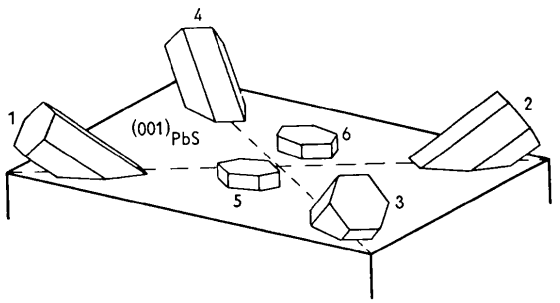


Fig. 4. Schematic depiction of epitaxies of α-CdS on galena cleavage face. The epitaxy involving four equivalent orientations, 1, 2, 3 and 4, is important in the present study.

β-CdS is formed (Figs. 5 and 6). Its cubic lattice is parallel to that of the substrate; i.e.

$$\{001\}_{\beta\text{-CdS}} \,//\, \{001\}_{\text{PbS}}$$
$$\langle 100\rangle_{\beta\text{-CdS}} \,//\, \langle 100\rangle_{\text{PbS}} .$$

In addition, thus orientated β-CdS is invariably accompanied by twins with respect to $\langle 111\rangle_{\beta\text{-CdS}}$ (polar axes), which are parallel to $\langle 111\rangle_{\text{PbS}}$. Thus, the polar axis of α-CdS in its dominant epitaxy and that of β-CdS are both parallel to $\langle 111\rangle_{\text{PbS}}$. Since the polar axis is normal to the above-mentioned unit layers to be stacked, this is a favourable situation for the electron diffraction to detect stacking fault, if the beam is along $\langle 110\rangle_{\text{PbS}}$.

(4) Experiments using mixed solutions with widely

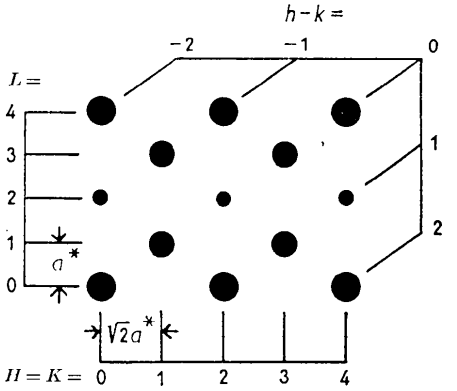


Fig. 6. Reciprocal lattice points of β-CdS. The plane of paper is $(\bar{1}10)$. Regarding the areas of circles, see the legend for Fig. 3. Regarding *HKL* and *hk*, see Section 3, (5).

varied ratios of $[NO_3]/[Cl]$, $[NO_3]/[Br]$, $[SO_4]/[Cl]$ and $[SO_4]/[Br]$ were carried out. When one of the above ratios is increased from 0 to ∞, the structure of the precipitate must change from α- to β-CdS. It was found that the transition is gradual, and that the precipitate at an intermediate stage consists generally of both α- and β-CdS components. Moreover, at an intermediate stage some of diffraction spots (in Fig. 7, e.g., those on the line marked) elongate along the *c*-axis. This suggests the occurrence of stacking faults (see below). It is worthy of note that such transient crystals involving stacking faults are formed at remarkably high values of the above four ratios (especially high for $[NO_3]/[Cl]$ and $[NO_3]/[Br]$). This implies that the effectiveness of halides in precipitating cadmium sulphide in α-form exceeds remarkably that of nitrate or sulphate in precipitating it in β-form. However, detailed accounts of this point will not be given in the present report.

(5) In Fig. 8, extracts from Figs. 2, 5 and 7, and from other diffraction patterns showing clear spot elongations due to stacking faults are assembled. Each extract involves a same line with $h-k\neq 0$ in the reciprocal space (the line marked in Fig. 7), where *hk* are either ordinary (two-layer) hexagonal indices or 'unit-layer hexagonal indices'. Note that *hk* are common to both hexagonal systems. The transformation equations between cubic *HKL* and unit-layer hexagonal *hk·l* are

$$\begin{cases} h = -H/2+K/2 \\ k = \quad -K/2+L/2 \\ l = \quad H/3+K/3+L/3 . \end{cases}$$

The abscissa $A_3$ of Fig. 8 is the variable in the reciprocal space, expressed in degree ($A_3=360^\circ\times l$). Intensity distributions along the line in Figs. 8(*a*)-(*f*) are respectively shown in Figs. 9(*a*)-(*f*). In obtaining these microphotometer records, the light beams were kept considerably narrow, in order to avoid confusion arising from effects other than stacking fault.

### 4. Various cases of one-dimensionally disordered close-packed structures

As far as a structure remains in close-packed states, diffraction spots on the line with $h-k=0$ (mod 3) show no elongations due to stacking fault (e.g., Guinier, 1956); elongations along the $c$-axis are confined to the spots on the lines with $h-k\neq 0$ (mod 3).

A stacking fault is referred to as a 'growth fault', if it is such that is encountered in crystal growth, i.e., if it produces a twinning. The diffraction theory of 'growth fault' should depend on its 'Reichweite', $s$ (Jagodzinski, 1949*a*), i.e. the number of layers preceding a given layer, which are effective in determining the lateral position of the given layer. For a structure to be close-packed, $s \geqq 1$ is necessary. Generally $2^{s-2}$ probabilities for faulty sequences take place.

The 'growth fault' with $s=1$ is so simple that it deserves hardly the term 'growth fault', constituting the most random case of close-packing (Jagodzinski, 1949*a*; Guinier, 1956). No fault probabilities are necessary to describe this structure, apart from the definite probability of $\frac{1}{2}$ for either $A \rightarrow B$ or $A \rightarrow C$ sequence, where $A$, $B$ and $C$ represent as usual three possible lateral positions in close-packing. Therefore, it does not account for a transition of a crystal between hexagonal and cubic structure according to experimental condition.

The theory of the 'growth fault' with $s=2$ in hexagonal or cubic close-packing was dealt with by Wilson (1942), Hendricks & Teller (1942) and Paterson (Appendix II in his paper, 1952). As the fault probability, say $\alpha$, in hexagonal close-packing increases from 0 to 1, it changes gradually from hexagonal to cubic, and *vice versa*.

The general theory of the 'growth fault' with $s=3$ in close-packing was dealt with by Jagodzinski (1949*b*). There take place two probabilities for faulty sequences:

$$h\begin{cases}\nearrow k:\alpha\\ \searrow h:1-\alpha\end{cases} \quad \text{and} \quad k\begin{cases}\nearrow k:\beta\\ \searrow h:1-\beta\end{cases},$$

where $h$ represents three consecutive layers arranged as in hexagonal close-packing, and $k$ those arranged as in cubic close-packing. The fraction of the hexagonal stacking sequence in the crystal is given by

$$w_h = (1-\beta)/(1+\alpha-\beta)\,.$$

By choosing various combinations of $\alpha$ and $\beta$, variously disordered states can be discussed, including necessarily the above cases of $s=2$ and $s=1$ as special cases (see below). 'Growth faults' with larger $s$ were also dealt with by Gevers (1954*a*, *b*).

On the other hand, if in an extended block of a crystal based on any pattern, regular or irregular, one half moves relative to the other, a different type of stacking fault arises. This should be discriminated from the 'growth fault' (Barrett, 1952; Paterson, 1952), and is referred to as a 'deformation fault'. 'Deformation faults' in cubic close-packing, in hexagonal close-packing, and in other complex close-packings were dealt with, respectively, by Paterson (1952) and Warren & Warekois (1955), by Christian (1954), and by Gevers (1954*a*). As the deformation fault probability, say $\alpha$, increases from 0 to 1, the crystal changes gradually to the twin of its original crystal.

Although a more general treatment covering both types of faults has been developed (Kakinoki *et al.*, 1955; Kakinoki, 1961), the above survey of the theories will be useful for interpretation of the present results. Many experimental works on structures involving stacking faults are reviewed by Jagodzinski (1949*c*), Warren (1959) and Kakinoki (1961).

### 5. Interpretation of results

The cadmium sulphide precipitates obtained as above show no appreciable transformations after being kept in a desiccator for several months. Therefore, what are being observed in this study are atomic structures as grown of the precipitates. Although $\alpha$-CdS is said to be the stable modification at room temperatures (Rittner & Schulman, 1943), $\beta$-CdS seems also to be practically stable at the temperatures. Since, moreover, the specimens are not subjected to any mechanical works, the theories to be considered for interpretation of the results do not seem to lie in those regarding 'deformation faults', but those regarding 'growth faults'.

According to Kakinoki *et al.* (1955) and Kakinoki (1961), with a single-crystal involving 'growth faults' intensity distributions on the lines with $h-k=\pm 1$ (mod 3) are both invariably symmetric with respect to $l=0$, and equal to each other, while with a single-crystal involving 'deformation faults' they are both generally asymmetric with respect to $l=0$ in such a way that one in the $+l(-l)$ direction is equal to the other in the $-l(+l)$ direction. However, the intensity distributions observed should not be compared directly with these intensity distributions, since the orientation of the precipitated crystallites under consideration is not single-crystalline, but four-crystalline. Nevertheless, by taking into account corrections arising from the four-crystal situation, such as in the next paragraph, it is confirmed that stacking faults in question are of 'growth' in nature.

The corrections necessary for comparison of the intensity distributions on the line with $h-k=-1$ (Figs. 8 and 9) with those deduced from the theories are illustrated for two simple cases in Fig. 10. Because of the presence of the four equivalent orientations, spot intensities due to single-crystalline $\alpha$- and $\beta$-CdS shown in Fig. 10(*a*) turn into those shown in Fig. 10(*b*). By comparing Fig. 10(*b*, 1) with Fig. 10(*a*, 1), and Fig. 10(*b*, 2) with Fig. 10(*a*, 4), it is seen that corrections of spot intensities are necessary only at $A_3 = 240°$ (mod 360°).

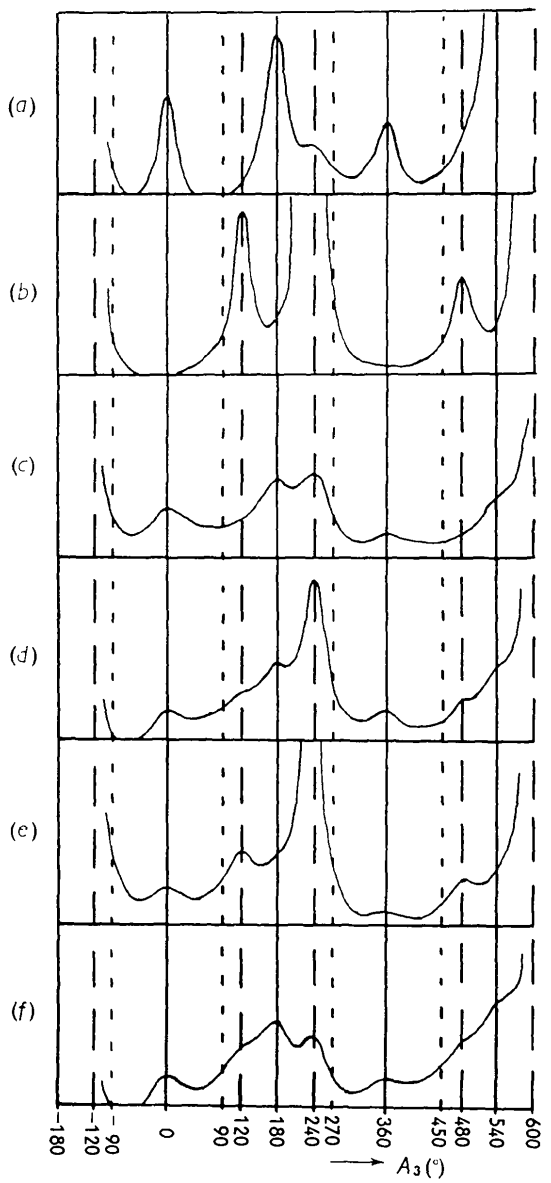


Fig. 9. Microphotometer records of Fig. 8. (*a*) to (*f*) correspond respectively to (*a*) to (*f*) of Fig. 8. Minor irregularities due to emulsion grains are eliminated.

In Figs. 2 and 5, which are respectively due to $\alpha$- and $\beta$-CdS, both purest possible under present experimental conditions, the spots are already diffuse to some extent, and, moreover, have particular shapes. These are understood as effects of particle size and shape, and of stacking faults arising to a minor extent even under these experimental conditions. Nevertheless, their intensity distributions on the line with $h-k=-1$ (Figs. 8(*a*) and (*b*); Figs. 9(*a*) and (*b*)) are qualitatively in harmony with Figs. 10(*b*, 1) and (*b*, 2), respectively. (A minor peak at 240° in Fig. 9(*a*) is due to a spot arising from the other unimportant orientation.)

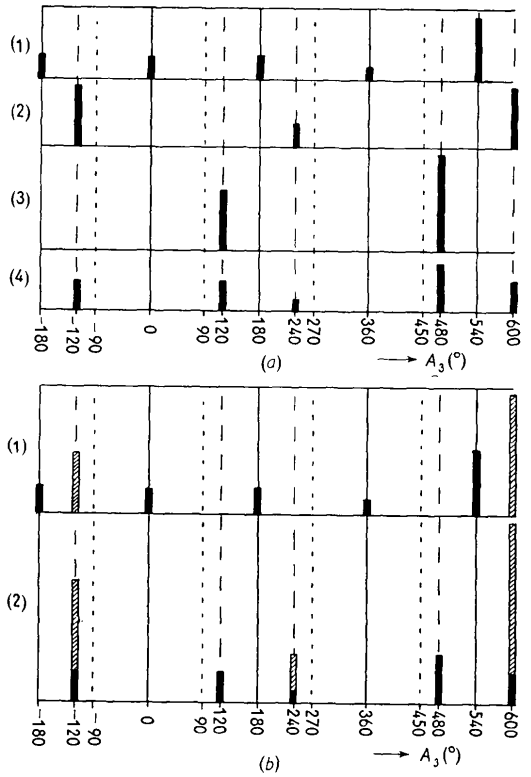


Fig. 10. Relative spot intensities on the line with $h-k=-1$ for (*a*) single-crystalline and (*b*) four-crystalline CdS. (*a*, 1) $\alpha$-CdS, (*a*, 2) $\beta$-CdS, (*a*, 3) twin of $\beta$-CdS of (*a*, 2), (*a*, 4) $\beta$-CdS containing 50% twin, (*b*, 1) $\alpha$-CdS, and (*b*, 2) $\beta$-CdS containing 50% twin. In (*b*, 1) and (*b*, 2) the intensities to be added by the four-crystal situation are shown by hatching. Note that, in contrast to the intensities shown by thick solid lines, those shown by hatching are not distributed along the abscissa (the line with $h-k=-1$), even if stacking faults take place. For the calculations, the scattering factors of Cd and S are both assumed to be constant and proportional to their atomic numbers.

Intensity distributions of Figs. 8(*c*)–(*f*) or Figs. 9(*c*)–(*f*) show that the spots on the line are generally more elongated than those of Figs. 8(*a*) and (*b*), or Figs. 9(*a*) and (*b*). This implies that the one-dimensional disorder is introduced to the specimens to remarkable extents during precipitation. That all the peaks other than at 240° exhibit elongations of the same order implies that these specimens are not, at least to the first approximation, simple mixtures of differently disordered crystallites, but they are quite uniform with respect to one-dimensional disorder; stacking fault probability or probabilities, depending on the composition of the solution used, seem to remain constant throughout the process of precipitation.

With the specimens disordered remarkably there are generally four intensity peaks in the range 0°–360° on the line with $h-k=-1$ (Figs. 8(*c*)–(*f*); Figs. 9(*c*)–(*f*)). The theory necessary and sufficient for accounting for this seems to lie in Jagodzinski's theory (1949*b*) regarding the 'growth fault' with $s=3$, touched upon in the foregoing section.

According to him, if particle size is sufficiently large, the intensity distribution along $h-k\neq 0 \pmod 3$ is given by

$$I=\tfrac{3}{2}|F|^2\times\left\{\frac{K_2(1-x_2^2)}{1-2x_2\cos A_3+x_2^2}+\frac{K_3(1-x_3^2)}{1-2x_3\cos A_3+x_3^2}\right.$$
$$\left.+\frac{A(1-\varrho^2)}{1-2\varrho\cos(A_3+\varphi)+\varrho^2}+\frac{A(1-\varrho^2)}{1-2\varrho\cos(A_3-\varphi)+\varrho^2}\right\},$$

where $F$ is the structure factor of the unit layer (Sections 1 and 3), $A_3$ is $360°\times l$ as before, and $x_2$, $K_2$, $x_3$, $K_3$, $\varrho$, $\varphi$, and $A$ are constants, depending on the two growth-fault probabilities, $\alpha$ and $\beta$ (Section 4). In the range 0°–360° of $A_3$, the first term in the braces becomes a maximum at 0° (or 360°), the second a maximum at 180° (since $x_3$ is invariably negative), the third a maximum at $360°-\varphi$, and the last a maximum at $\varphi$. The first two terms correspond to the spots of $\alpha$-CdS (two-layer structure), and the last two to those of $\beta$-CdS (three-layer structure), if $\varphi=120°$. Jagodzinski (1949*b*) calculated and listed the above seven constants for twenty-five combinations of $\alpha$ and $\beta$ ($\alpha$ or $\beta=0{\cdot}1$, 0·3, 0·5, 0·7, or 0·9). From these constants and $F$ for cadmium sulphide, intensity distributions for these cases are readily calculated. Some of the results of calculations are illustrated in Fig. 11.

Fig. 12 will be convenient for surveying many cases involved in the theory. The twenty-five cases are located at the intersecting points of five vertical and five horizontal lines. The thick lines represent various fractions $w_h$ of the hexagonal stacking sequence (Section 4). Structures in the region close to the left-hand side are nearly hexagonal, becoming purely hexagonal on the left-hand side (excluding the left upper corner), whereas those in the region close to the upper side are nearly cubic, becoming purely cubic on the upper side (excluding the left upper corner). In structures in the left upper region, the faulty sequences, $h\rightarrow k$ and $k\rightarrow h$, are comparatively rare, the structure at the left upper corner becoming a simple mixture of purely hexagonal and purely cubic structures, the mixing ratio being arbitrary. Therefore, intensity peaks appear generally at or near 0°, 120°, 180° and 240° (all mod 360°) for structures in the left upper region (Fig. 11(*a*)). On the contrary, in structures in the right lower region, the faulty sequences are comparatively frequent, the structure at the right lower corner becoming a four-layer structure. Therefore, intensity peaks at or near 90° and 270° (both mod 360°) are characteristic to structures in the right lower region (Fig. 11(*c*)).

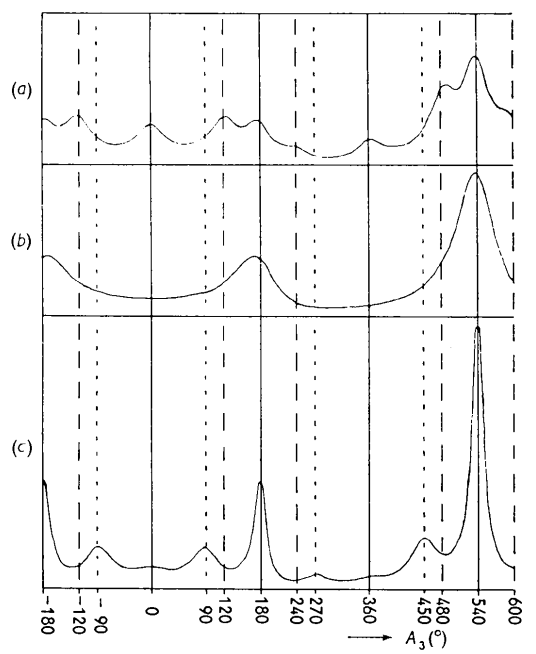


Fig. 11. Examples of relative intensity distributions along $h-k\neq 0 \pmod 3$ of single-crystalline CdS according to Jagodzinski's theory. (*a*) $\alpha=0{\cdot}3$, $\beta=0{\cdot}7$, (*b*) $\alpha=0{\cdot}5$, $\beta=0{\cdot}5$, (*c*) $\alpha=0{\cdot}7$, $\beta=0{\cdot}3$. For all $w_h=0{\cdot}5$. For the calculations, the scattering factors of Cd and S, located respectively at (0, 0, 0) and at (0, 0, ½), are both assumed to be constant and proportional to their atomic numbers.

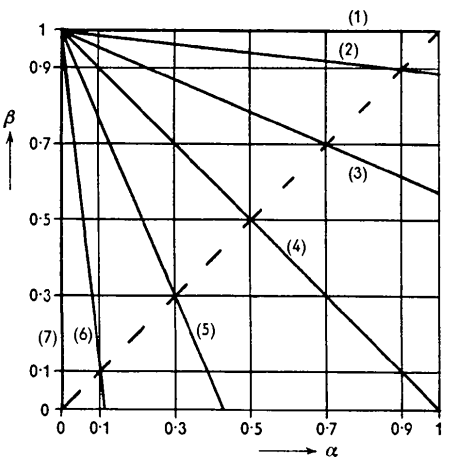


Fig. 12. Various cases involved in the theory regarding 'growth fault' with $s=3$. Jagodzinski's 25 cases are the combinations of $\alpha$ or $\beta=0{\cdot}1$, 0·3, 0·5, 0·7, or 0·9. Values of $w_h$ are constant on thick lines: (1) 0, (2) 0·1, (3) 0·3, (4) 0·5, (5) 0·7, (6) 0·9, and (7) 1. The 'Reichweite' of 3 turns into 2 on the broken line, $\alpha=\beta$, and into 1 at the point, $\alpha=\beta=0{\cdot}5$.

The structures at the four corners of Fig. 12 are expressed by notations for regular stackings by Jagodzinski (1949*a*) and Wyckoff (1960), by Ramsdell (1944, 1945, 1947), by Zhdanov (1945), and by Frank (1951), as in the following respective ways:

| | |
|---|---|
| left lower corner (and left-hand side): | $h$, $2H$, 11, △▽ |
| right upper corner (and upper side): | $k$, $3C$, 10, △ |
| left upper corner: | simple mixture of the above two |
| right lower corner: | $hk$, $4H$, 22, △△▽▽ . |

It is to be noted that the last four-layer structure has the longest possible regular period in Jagodzinski's theory.

On the broken line expressing $\alpha=\beta$ in Fig. 12, the theory degenerates to one regarding $s=2$ (Section 4), where only either the first two or the last two terms in the formula for $I$ remain. Therefore, for structures on the broken line generally only two intensity peaks appear in the range 0°–360°. Moreover, at the point on the broken line, where $\alpha=\beta=0{\cdot}5$, the theory degenerates again to one regarding $s=1$ (Section 4), where only the second term remains, leading to a single intensity peak in the range 0°–360°. Since this is the case of the most random close-packing, spot elongations are most pronounced (Fig. 11(*b*)). Thus, the feature of $I$ for any combination of $\alpha$ and $\beta$ can be predicted in outline from where it is located in Fig. 12. Indeed, Fig. 11 and other results of numerical calculations of $I$ for Jagodzinski's twenty-five cases are in harmony with these predictions. Conversely, $\alpha$, $\beta$ and $w_h$ of a specimen can be deduced, at least approximately, from the intensity distribution along $h-k\neq 0 \pmod 3$ in its diffraction pattern, if it is compared with the above calculations.

Now, in Figs. 8(*c*)–(*f*) and Figs. 9(*c*)–(*f*) the intensity peaks in the range 0°–360°, generally four in number, are located at or very close to 0° (or 360°), 120°, 180°, or 240°; all of them are peaks due to $\alpha$-like and $\beta$-like structures. No cases with peaks at or very close to 90° or 270°, due to the above four-layer like structures, have been encountered throughout the experiments. This implies that the precipitates disordered remarkably under the present experimental conditions are invariably in the left upper region of Fig. 12, where the faults are comparatively rare. For example, in the specimen of Fig. 8(*f*) or Fig. 9(*f*), whose $w_h$ seems to be approximately 0·5, the fault probabilities seem to be approximately $\alpha=0{\cdot}3$, $\beta=0{\cdot}7$. This will be understood from the comparison of Fig. 9(*f*) with Fig. 11(*a*), if the correction due to the four-crystal situation, simple cases of which are illustrated in Fig. 10, is taken into account.

It is concluded, therefore, that with increasing ratio of $[NO_3]/[Cl]$, $[NO_3]/[Br]$, $[SO_4]/[Cl]$, or $[SO_4]/[Br]$ from 0 to $\infty$, the fault probabilities, $\alpha$ and $\beta$, of the precipitate move in Fig. 12 from somewhere close to the left-hand side through a path in the left upper region to somewhere close to the upper side. What underlies this conclusion lies most likely in the situation that $\alpha$- and $\beta$-CdS are both stable, at least practically, at room temperatures; the faulty sequences, $h\rightarrow k$ and $k\rightarrow h$, seem to require comparatively high energies.

It is to be added that the experimental results can be also qualitatively accounted for on the basis of a theory with larger $s$, if the fault probabilities are specially chosen. In the theories with larger $s$, there appear many intensity peaks expressed by terms similar to those in the above formula for $I$ (Jagodzinski, 1949*b*; Gevers, 1954*a*, *b*). Therefore, in order to account for the present results, the probabilities, $2^{s-2}$ in number, must be so chosen as to make all the peaks other than the above four almost vanish. This means that the theory approaches to one with $s=3$. It can be said, therefore, that the 'Reichweite' necessary and sufficient for crystallographic description of one-dimensionally disordered precipitates of cadmium sulphide is practically 3.

Although the particle size effect requires a correction for the formula for $I$, it is not serious for the particle size of about 100 Å. It does not modify essentially, therefore, the qualitative interpretation carried out so far.

## 6. Discussion

The present study has thus shown that structures of cadmium sulphide precipitates are described practically on the basis of the theory regarding 'growth fault' with $s=3$. Although this may be also expected with natural zinc sulphides, i.e. wurtzite and zinc blende, Jagodzinski (1949*c*) showed that this is not the case with wurtzite. The deviation from the expectation was ascribed by him to the situation that the inherent 'growth faults', introduced at the stage of crystal formation, serve as embryos for subsequent transformation to zinc blende, the resulting faults becoming not of pure 'growth'. Since zinc blende is the only stable modification at room temperatures, his interpretation seems to be tenable.

With silicon carbide, occurrence of numerous polytypes with long regular stacking period along the *c*-axis is remarkable. The regular period of as many as 594 layers is reported (Honjo *et al.*, 1950). Many works in this field are reviewed by Jagodzinski & Arnold (1960), Amelinckx & Strumane (1960), and Verma (1960). Since the present knowledge of atomic interaction in crystal lattices is confined to forces of short range order, the occurrence of the numerous long periods is hardly conceivable. In order to overcome this difficulty, Frank (1951, 1952) and Verma (1951, 1953, 1960) paid attention to growth steps of screw dislocations during growth, Jagodzinski (1954*a*, *b*) introduced the conception of vibration entropy, and Schneer (1955) treated the phase transformation as a cooperative phenomenon.

In contrast to the above complicated cases of zinc sulphide and silicon carbide, the present case of cadmium sulphide precipitates is fortunately much simpler. Their structures are in the states as grown, since $\alpha$- and $\beta$-CdS are both stable, at least practically, at room temperatures. In such a case the 'Reichweite' will have a direct bearing on the interatomic force during crystal formation. It is remarkable that the 'Reichweite' required for description of the intermediate states between $\alpha$- and $\beta$-CdS is at least 3, although intermediate states between them on the basis of $s=2$ are crystallographically possible on the broken line in Fig. 12. The transition between them

through a path, where the faults are comparatively rare, can be understood reasonably from the stability of both modifications.

In addition to the present study utilizing electron diffraction, an X-ray diffraction study of cadmium sulphide powders predipitated chemically is under way. The results obtained up to date are compatible with those of the present report.

This paper is published by permission of Mitsubishi Metal Mining and Metallurgical Laboratory.

### References


AMELINCKX, S. & STRUMANE, G. (1960). *Silicon Carbide*, p. 162. (Ed. by O'Connor, J. R. & Smiltens, J.). London: Pergamon.

BARRETT, C. S. (1952). *Imperfections in Nearly Perfect Crystals*, p. 97. (Ed. by Schockley, W. *et al.*). New York: Wiley.

CHRISTIAN, J. W. (1954). *Acta Cryst.* **7**, 415.

FRANK, F. C. (1951). *Phil. Mag.* **42**, 1014.

FRANK, F. C. (1952). *Ad. Phys.* (*Phil. Mag. Suppl.*), **1**, 91.

GEVERS, R. (1954*a*). *Acta Cryst.* **7**, 337.

GEVERS, R. (1954*b*). *Acta Cryst.* **7**, 492.

GUINIER, A. (1956). *Théorie et Technique de la Radiocristallographie*, Chap. 13. Paris: Dunod.

HENDRICKS, S. & TELLER, E. (1942). *J. Chem. Phys.* **10**, 147.

HONJO, G., MIYAKE, S. & TOMITA, T. (1950). *Acta Cryst.* **3**, 396.

JAGODZINSKI, H. (1949*a*). *Acta Cryst.* **2**, 201.

JAGODZINSKI, H. (1949*b*). *Acta Cryst.* **2**, 208.

JAGODZINSKI, H. (1949*c*). *Acta Cryst.* **2**, 298.

JAGODZINSKI, H. (1954*a*). *Acta Cryst.* **7**, 300.

JAGODZINSKI, H. (1954*b*). *Neues Jahrb. Min.* **3**, 49.

JAGODZINSKI, H. & ARNOLD, H. (1960). *Silicon Carbide*, p. 136. (Ed. by O'Connor, J. R. & Smiltens, J.). London: Pergamon.

KAKINOKI, J. (1961). *X-ray Crystallography*, Vol. 2, Part IV, Chap. 5 (in Japanese). (Ed. by Nitta, I.). Tokyo: Maruzen.

KAKINOKI, J., KOMURA, Y. & HIZIYA, K. (1955). *X-rays*, **8**, 67 (in Japanese).

MILLIGAN, W. O. (1934). *J. Phys. Chem.* **38**, 797.

PATERSON, M. S. (1952). *J. Appl. Phys.* **23**, 805.

RAMSDELL, L. S. (1944). *Amer. Min.* **29**, 431.

RAMSDELL, L. S. (1945). *Amer. Min.* **30**, 519.

RAMSDELL, L. S. (1947). *Amer. Min.* **32**, 64.

RITTNER, E. S. & SCHULMAN, J. H. (1943). *J. Phys. Chem.* **47**, 537.

SATO, R. (1953*a*). *J. Phys. Soc. Japan*, **8**, 152.

SATO, R. (1953*b*). *J. Phys. Soc. Japan*, **8**, 454.

SATO, R. (1954). *J. Min. and Metall. Inst. Japan*, **70**, 359 (in Japanese).

SATO, R. (1955). *J. Appl. Phys. Japan*, **24**, 413 (in Japanese).

SATO, R. (1957). *Proc. Second Internat. Congr. Surface Activity*, Vol. 3, p. 349. (Ed. by Schulman, J. H.).

SATO, R. (1959). *Nature, Lond.* **184**, 2005.

SCHNEER, C. J. (1955). *Acta Cryst.* **8**, 279.

SWANSON, H. E., FUYAT, R. K. & UGRINIC, G. M. (1955). *Standard X-Ray Diffraction Patterns* (Circ. Nat. Bur. Stand., No. 539), **4**, 15.

TRAILL, R. J. & BOYLE, R. W. (1955). *Amer. Min.* **40**, 555.

VERMA, A. R. (1951). *Phil. Mag.* **42**, 1005.

VERMA, A. R. (1953). *Crystal Growth and Dislocations*, Chap. 7. New York: Academic Press.

VERMA, A. R. (1960). *Silicon Carbide*, p. 202. (Ed. by O'Connor, J. R. & Smiltens, J.). London: Pergamon.

WARREN, B. E. (1959). *Progress in Metal Physics*, Vol. 8, p. 147. (Ed. by Chalmers, B. & King, R.). London: Pergamon.

WARREN, B. E. & WAREKOIS, E. P. (1955). *Acta Metall.* **3**, 473.

WILSON, A. J. C. (1942). *Proc. Roy. Soc.* A, **180**, 277.

WYCKOFF, R. W. G. (1960). *Crystal Structures*, Vol. 1, Chap. 3. New York: Interscience.

ZHDANOV, G. S. (1945). *Dokl. Akad. Nauk. USSR*, **48**, 39.